JTTEE5 19:294–302
DOI: 10.1007/s11666-009-9443-x
1059-9630/$19.00 © ASM International

Peer Reviewed

Synthesis and Microstructure Evolution of Nano-Titania Doped Silicon Coatings

N.A. Moroz, H. Umapathy, and P. Mohanty

(Submitted April 26, 2009; in revised form September 17, 2009)

The Anatase phase of Titania (TiO_2) in nanocrystalline form is a well known photocatalyst. Photocatalysts are commercially used to accelerate photoreactions and increase photovoltaic efficiency such as in solar cells. This study investigates the in-flight synthesis of Titania and its doping into a Silicon matrix resulting in a catalyst-dispersed coating. A liquid precursor of Titanium Isopropoxide and ethanol was coaxially fed into the plasma gun to form Titania nanoparticles, while Silicon powder was externally injected downstream. Coatings of 75-150 μm thick were deposited onto flat coupons. Further, Silicon powder was alloyed with aluminum to promote crystallization and reduce the amorphous phase in the Silicon matrix. Dense coatings containing nano-Titania particles were observed under electron microscope. X-ray diffraction showed that both the Rutile and Anatase phases of the Titania exist. The influence of process parameters and aluminum alloying on the microstructure evolution of the doped coatings is analyzed and presented.

Keywords influence of spray parameters, nanostructured coatings, nanostructured materials, solution-precursor TS

1. Introduction

Recent focus in sources of alternative energy, such as solar power by using photovoltaic solar cells, has generated renewed interest in the photocatalytic applications of Titanium Dioxide (Titania) (Ref 1). Titania is a widely known and readily available photocatalyst. Titania's ability to absorb light energy makes it a viable material to implant in a matrix of crystalline Silicon in order to increase the efficiency of photovoltaic cells.

The increase in efficiency of the photovoltaic cell due to the embedded Titania particles is proportional to the surface area of the Titania (Ref 2). Therefore, nanoparticles of Titania are expected to yield a large surface area due to their small size, and still maintain the physical integrity of the Silicon. With respect to Titania, as the particle size reaches an optimal value of 10 nm, the surface charge carrier rate is high, aiding improvements in the photocatalytic efficiency (Ref 2). Hence, the synthesis of Titania particles in nanoscale are studied and investigated in this article.

There are three crystalline phases of Titania; Anatase, Rutile, and Brookite (Ref 3). Rutile is the stable phase of Titania, whereas Anatase is the metastable state. Brookite has a defective lattice structure, and hence, is not of much interest for improving the efficiency of photovoltaics (Ref 3). Anatase Titania can be irreversibly converted to stable Rutile phase by heat treatment. It has been shown (Ref 4) that the Anatase phase of Titania improves the photocatalytic property of the bulk coatings as compared to the Rutile phase of the Titania.

In earlier works (Ref 5-7), attempts have been made using plasma spray to produce Titania nanoparticle coatings that would show predominant Anatase phase. Though a fraction of the nanoparticles in the plasma plume showed indication of the Anatase phase, the coatings have nevertheless showed predominantly the Rutile phase (Ref 8).

Factors that determine the resultant phase of the Titania after pyrolysis via the plasma plume are primarily the temperature of the plasma, the flight distance of the particles, and the cooling rate of sprayed particles (Ref 6).

A proven method to produce nanoparticles of Titania and successfully feed them into a plasma plume is by creating a liquid precursor of Titania (Ref 5). The liquid precursor allows the transportation of nanoparticles into a pressurized gas flow, which would not be possible using conventional powder feeders. Liquid precursors can be in the form of suspensions, colloids, or solutions. Solutions form the desired particles in situ within the plume of the plasma gun, whereas suspensions and colloids have preformed particles which are modified by the plasma plume. For this application the precursor can be considered a

This article is an invited paper selected from presentations at the 2009 International Thermal Spray Conference and has been expanded from the original presentation. It is simultaneously published in *Expanding Thermal Spray Performance to New Markets and Applications: Proceedings of the 2009 International Thermal Spray Conference*, Las Vegas, Nevada, USA, May 4-7, 2009, Basil R. Marple, Margaret M. Hyland, Yuk-Chiu Lau, Chang-Jiu Li, Rogerio S. Lima, and Ghislain Montavon, Ed., ASM International, Materials Park, OH, 2009.

N.A. Moroz, H. Umapathy, and **P. Mohanty**, Additive Manufacturing Processes Laboratory, University of Michigan-Dearborn, 4901 Evergreen Road, Dearborn, MI 48128. Contact e-mails: nmoroz@umich.edu and u.harishankar@gmail.com.

suspension since the Titania particles are produced in the precursor before they are introduced to the plasma plume and there are Titania particles that exceed 1 μm. The particular setup used to obtain the coatings shown in this article was achieved by using a liquid Titania precursor injected in the plasma plume using two methods: internal, axially feeding of the precursor through an injector near the anode, and external, radial feeding of the precursor into the plume using a two fluid atomizing nozzle utilizing compressed air for atomization of the precursor. The feeding mechanisms are detailed in the Experimental Procedure.

The bulk coating is desired to have a matrix of crystalline Silicon with embedded Titania nanoparticles. For all setups the Silicon was fed externally into the plasma plume via two injectors using a conventional powder feeder. No protective atmosphere was used for any of the coating processes.

This article discusses the spray parameters and the experimental setup used to achieve a dense Silicon-Titania coating, with the Anatase phase of Titania nanoparticles predominantly observed in the coating. Previous research has yielded silicon coatings via plasma spray with void contents of 3-7% for dense layers and 50% void content for porous layers, used for antireflection layers (Ref 9-11). It was the goal of this article to achieve similar porosities for dense and porous layers of silicon. The SEM images and the XRD patterns of the spray coatings at the surface and the cross section are recorded and discussed.

2. Experimental Procedure

2.1 Materials

Silicon powder (99.99% Si, average size of 10 μm) was obtained from Atlantic Equipment Engineers (Bergenfield, NJ). The average powder particle size was observed to be 3.36 μm with a standard deviation of 5.97 μm using SEM and image analysis (Fig. 1). The large distribution of particle size did not appear to affect the feeding of the powder using the powder feeders.

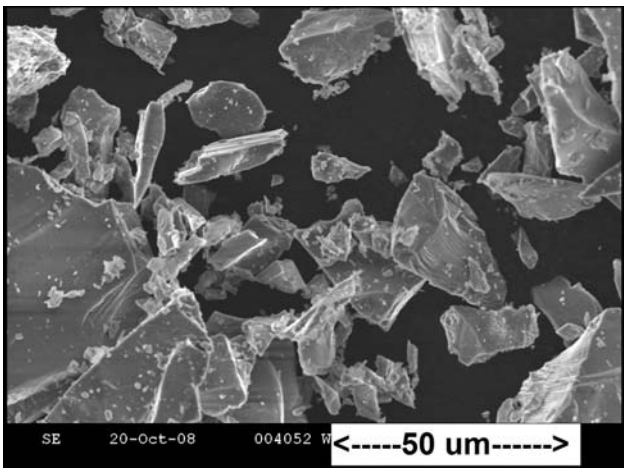

Fig. 1 SEM picture of Silicon powder (99.99%)

A suspension precursor of Titania was produced by mixing Titanium Isopropoxide (97%) with ethanol (99%) and water. Glacial acetic acid (99.8%) and hydrogen peroxide (3%) were used as dispersants. The ratio of Titanium Isopropoxide to water by volume in the precursor was varied throughout the experiment. Typically, 10-100 mL of Titanium Isopropoxide was added to 200-500 mL of ethanol and 5-10 mL of acetic acid and hydrogen peroxide. A composition of 20 mL of Titanium Isopropoxide, 10 mL of acetic acid, 5 mL of hydrogen peroxide, and 410 mL of ethanol produced the best results. The precursor was produced in an Erlenmeyer flask and constantly agitated using a magnetic stirrer. Titanium Isopropoxide was added to the flask of ethanol first, then acetic acid was added, and finally the hydrogen peroxide.

2.2 Plasma Spray Process

A 100-HE plasma gun (Progressive Technologies Inc., Grand Rapids, MI) was used to deposit the Silicon-Titania composite coating onto steel substrates. Two sets of experiments were performed with variations on the material feed process and plasma gun setup to determine the optimal conditions for a dense Silicon coating doped with Anatase phase Titania nanoparticles. The substrates used were $76 \times 50.8 \times 3.175$ mm^3 steel coupons. The coupons were grit blasted with aluminum oxide size 36-grit and no other pretreatment process was used. The typical spray distance is 120 to 200 mm. The steel coupons were cooled from the back by compressed air of pressure 80 psi. For efficient photocatalytic applications, coatings with void content less than 10% are vital and the target thickness of the coating was approximately 150 μm. Porosity in Silicon coatings increases the resistance of electron transfer, thereby reducing the photovoltaic efficiency (Ref 12).

The in-flight pyrolysis of the precursor for each setup was also investigated by spraying Titania particles directly into a beaker of distilled water with 154 mm spray distance as this is within the range of spray distance used for depositing the coatings onto steel substrates. By this procedure, the phase of the Titania particles was retained in anatase phase. Since quenching the molten Titania particles in anatase phase is the critical factor, this can be achieved by spraying the precursor in water. The only purpose of doing so is to measure the particle size. In case of spraying in steel substrate, the spray distance plays an important role, as the plasma plume ends up heating the substrate if the spray distance is too low. If it's too far, the particles end up cooling. This converts the meta stable anatase phase of titania into stable rutile phase. The water was evaporated using a furnace at 80 °C, and the remaining particles were characterized using SEM.

The temperature of the target surface of the substrate was recorded using a K-type thermocouple read by a programmable logic controller. The thermocouple was pressed to the target surface of the substrate 10 mm below the plasma plume. Average target surface temperature of

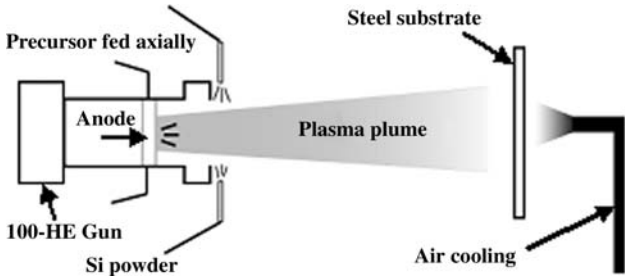

Fig. 2 Schematic of setup 1 showing externally fed Silicon powder and axially fed precursor through the anode of the 100-HE plasma gun

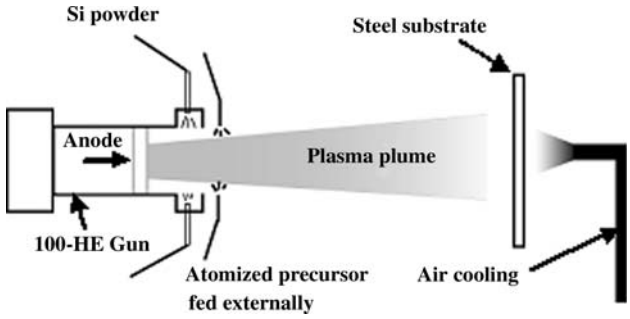

Fig. 3 Schematic of setup 2 showing externally fed Silicon powder and externally fed precursor introduced to the plume of the 100-HE plasma gun

Table 1 Plasma gun parameters for the two experimental setups

	Primary gas Ar, L/min	Secondary gas N_2, L/min	Ternary gas H_2, L/min	Voltage, V	Current, A
Setup 1	94.33	44.83	70.67	265	245
Setup 2	94.33	47.17	52.33	265	245

the substrate while spraying was determined to be 650 °C with compressed air cooling, without cooling the average temperature was determined to be 950 °C.

2.3 Setup 1: Axial Injection

An Axial extension head was used with the 100-HE plasma gun. The axial extension head allows feedstock to be fed coaxially into the plasma plume (Fig. 2). This setup is generally referred as setup 1, in this document.

In order to produce nanoparticles of Titania, the precursor needed to be atomized in the plasma plume. Thus, the precursor was introduced into the plume at the center of the extension head which has a hole of 12.7 mm. The injector has a nozzle diameter of 2 mm. The shear forces from the jet would then atomize the precursor. The Titania suspension precursor was fed into the injector with a peristaltic pump at a feedrate of 3-5 mL/min, resulting in 0.04-0.06 g/min of Titania into the plume. Silicon powder was externally fed into the plasma jet with a Plasmatron Roto (Navi Mumbai, Maharashtra, India) feed hopper set to 3 rpm with an argon carrier gas with a flow of 7 L/min. The spray distance varied between 150 and 230 mm. The substrate was cooled using compressed air at a pressure of 414-550 kPa. It can be noted that both nitrogen and hydrogen are used as secondary gases as listed in Table 1. The purpose of using these two diatomic gases is due to its high heating content, which was required to heat the silicon particles. Other plasma gun parameters are listed in Table 1.

2.4 Setup 2: Radial Injection

The 100-HE gun was used in its standard configuration (Fig. 3). This setup is generally referred as setup 2 in this document. The Titania suspension precursor was externally fed into the plasma plume with an atomizing nozzle (Koolmist, San Francisco, CA) with air as atomizing gas at a pressure of 200 kPa. The Silicon powder was also externally fed into the plasma jet with a Plasmatron Roto feed hopper set to 3 rpm with an argon carrier gas flow of 7 L/min. The spray distance varied between 150 and 230 mm. The substrate was cooled using compressed air at a pressure of 414-550 kPa. Other gun parameters are listed in Table 1.

2.4.1 Characterization. The topology of the coated substrates was examined using SEM (Hitatchi S-2600N) and AFM (Q-Scope 250). XRD (Rigaku MiniFlex) was also performed on the coatings to determine the crystalline structure of the Silicon matrix and as well as the Titania particles. The XRD setup used had a Cu-K_α anti cathode and the wavelength is 1.54 Å. The substrates were also cut using wet abrasive cutoff saw and the cross sections of the coatings were analyzed using SEM to determine the uniformity of dispersion of the Titania nanoparticles in the Silicon matrix. The cross sections were polished with lapping discs of aluminum oxide with grit sizes of 240, 400, 600, 800, and 1200. The total void content of the coatings was calculated by image analysis using PaxCam software (PaxCam, Villa Park, IL). SEM images of the cross sections of the coatings were taken at 1000× magnification to use with the PaxCam software to determine void content.

3. Results and Discussion

3.1 Deposition of Crystalline Silicon

For a polycrystalline silicon photovoltaic cell, the matrix of Silicon must be predominantly crystalline (Ref 12). The morphology, porosity, deposition rate, and crystalline structure of Silicon for each setup were investigated by spraying a series of samples without the Titania precursor. Both setups 1 and 2 externally fed the Silicon powder into the plasma plume using a standard rotating wheel powder feeder described earlier with argon as a carrier gas. The plasma gun power, spray distance, and sample cooling techniques were varied to determine the

Table 2 Comparison of Silicon deposition of setups 1 and 2

	Spray distance, mm	Gun power, kW	Cooling air, kPa	Deposit rate, µm/pass	Void content, %	Plasma transverse speed, mm/s
Setup 1	150-230	65	414-550	0.254	<5	200
Setup 2	150-230	65	414-550	0.254	<5	200

Both setups accomplished the crystalline phase of Silicon

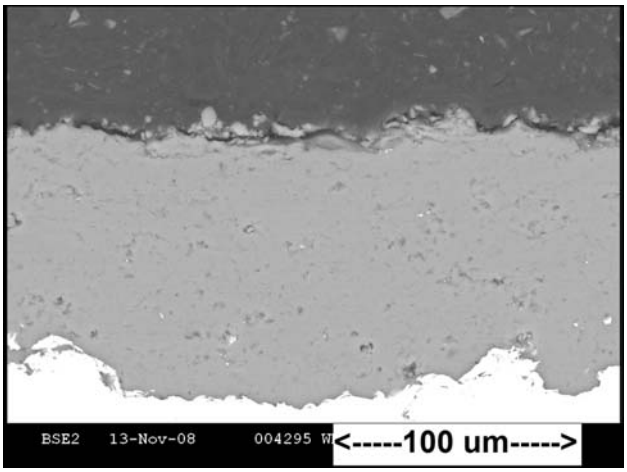

Fig. 4 Cross section SEM image of externally fed Silicon coating using setup 1

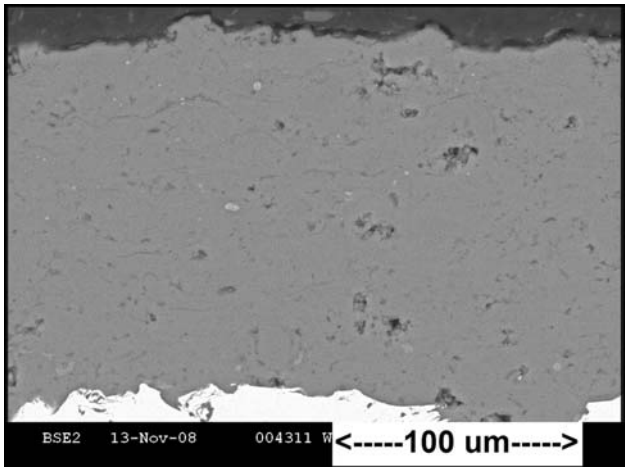

Fig. 5 Cross section SEM image of externally fed Silicon coating using setup 2

optimal conditions to achieve a crystalline Silicon structure. Spray distance and plasma gun power showed negligible change to the coating morphology or the deposition rate. Compressed air at 414-550 kPa was applied to the back of the sample which prevented cracking of the Silicon coating due to thermal stresses from the expansion of the steel sample. The substrate reached 1000 °C during deposition and was cooled to room temperature after deposition using a jet of compressed air pointed to the other side of the coating surface. Using the parameters shown in Table 1 and 2 yielded a deposition rate of 0.254 µm/s, which is equivalent to 0.254 µm/pass, of Silicon for setup 1 as well as for setup 2.

SEM and XRD were performed on the coatings, which verified that the Silicon has indeed fused completely and formed a relatively dense coating and was also in the crystalline form. Figures 4 and 5 show the SEM images of the cross sections of the Si coatings obtained using setups 1 and 2.

Figure 6 shows the XRD pattern of the Si coating. The void content of the Silicon coating was estimated to be less than 5% for each coating using image analysis. The void content values measured by this technique seemed to be influenced by the craters formed during sample polishing preparation. Typically voids formed during the consolidation of the droplets would have smooth edges. However, as seen in Fig. 4 and 5, many of the craters have rough edges indicating a brittle fracture. Therefore, it is believed that the actual void content in these coatings is lower than the value measured by image analysis. Both

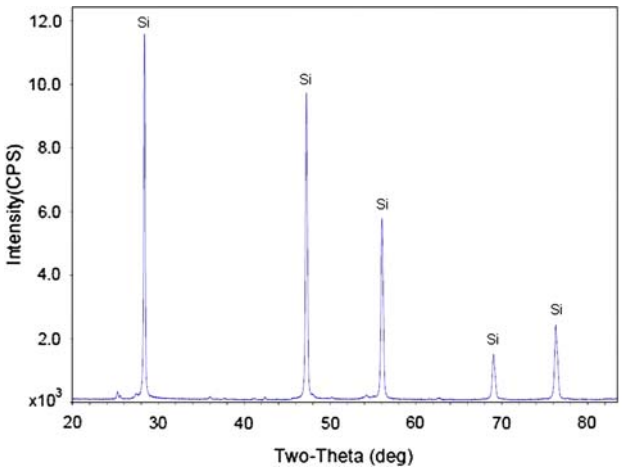

Fig. 6 XRD pattern of Silicon coatings from setup 1 showing the presence of the crystalline phase of Silicon

morphologies appear to be very similar. The two setups also showed negligible difference in deposition rate or void content.

Using the experimental setup, it was possible to produce both porous and dense Si coatings. A dense coating is required for higher photocatalytic efficiency as the porous structure increases the resistance for electron transfer (Ref 10). Any and all voids inhibit electron transfer, regardless of their size or shape. Dense coatings of Si can also be utilized as sputtering targets for PVD and CVD

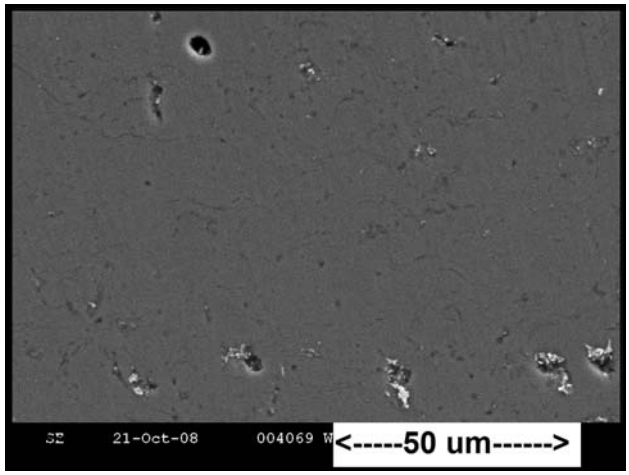

Fig. 7 Dense Si coating produced using setup 1

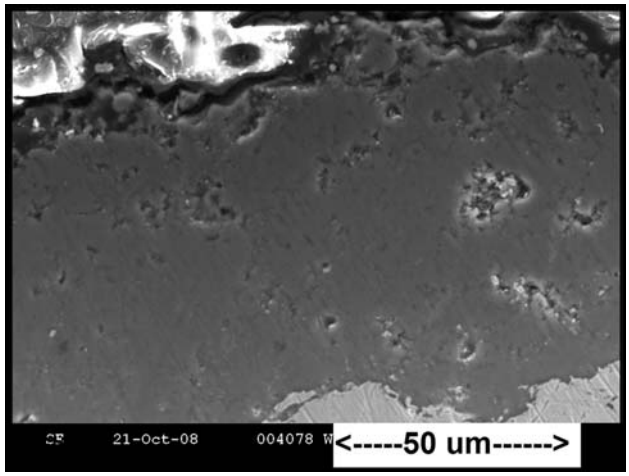

Fig. 8 Porous Si coating produced using setup 1

processes as porosity in sputtering targets leads to unstable sputtering and decrease in the coating quality (Ref 13). Porous coatings can be used as antireflection coatings in Si photovoltaic converters (Ref 14). Hence, there is commercial interest in producing both porous and dense Si coatings, to which plasma spray is applicable to control the porosity of the Si coatings. A fairly dense and porous Si coatings are shown in Fig. 7 and 8. No silica or other oxidation was seen in the coating. The lack of oxidation is most likely due to the accelerated quenching time of the coating and the low substrate temperature.

It has been demonstrated that the presence of aluminum assists the crystallization of silicon and the term ''aluminum-assisted crystallization'' has appeared in literature (Ref 15). Coatings with aluminum powder, ~10% by volume and silicon powder were blended together and fed into the plasma gun using the regular powder feed system used previously. The coatings sprayed with aluminum added to the silicon showed no real gain in crystallization compared to the coatings using exclusively

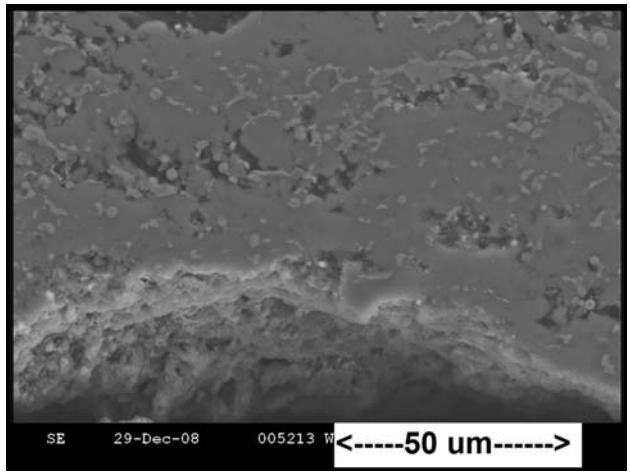

Fig. 9 Si-TiO_2 coating with Titanium Isopropoxide to water ratio of 0.3:1.0

silicon powder. The substrates were cooled at the back with compressed air. Hence, a heated substrate is not the reason for no improvements in crystallinity of silicon. All the peaks of silicon in the XRD graphs matched with both the silicon and Si-Al mixed coatings. Since the pure Silicon coatings were found to be overwhelmingly crystalline, alloying with aluminum was deemed unnecessary and abandoned.

3.2 Effect of Titanium Isopropoxide to Water Ratio

The chemical reaction between liquid water and TiISO is defined as in Eq (1) (Ref 16).

$$\mathrm{Ti}\{\mathrm{OCH(CH_3)_2}\}_4 + 2\mathrm{H_2O} \rightarrow \mathrm{TiO_2} + 4(\mathrm{CH_3})_2\mathrm{CHOH} \quad \text{(Eq 1)}$$

Thus, H_2O acts as a limiting reagent before the pyrolysis of the Titanium Isopropoxide in the plasma plume. The ratio of Titanium Isopropoxide to H_2O in the precursor was varied in order to determine if it affected the size of the nanoparticles of Titania produced within the plasma plume. The results of coatings produced using Titanium Isopropoxide to water ratios of 0.3:1.0, 0.45:1.0, 0.9:1.0 are shown in Fig. 9, 10, and 11, respectively. It can be observed that the size and the quantity of the Titania particles in the coatings increase as the concentration of the water is increased. This is due to the increase in the formation and agglomeration of the Titania as more water is available.

3.3 In-Flight Particle Characterization

The in-flight size of the Titania particles was examined by spraying directly into a beaker of distilled water. After the water was evaporated, the particles were examined using SEM (Fig. 12).

For both setups, it was confirmed using SEM that majority of the in-flight particles of Titania is in 100-200 nm in size using a TiISO to water ratio of 0.45:1.0.

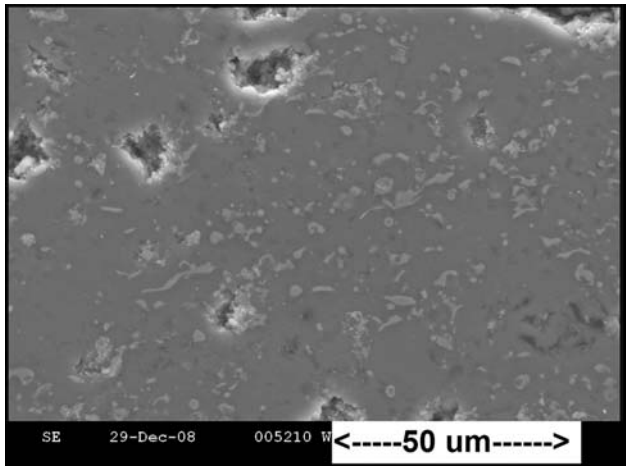

Fig. 10 Si-TiO_2 coating with Titanium Isopropoxide to water ratio of 0.45:1.0

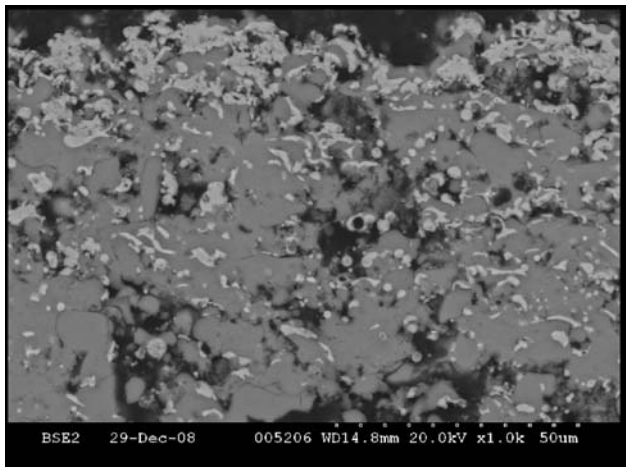

Fig. 11 Si-TiO_2 coating with Titanium Isopropoxide to water ratio of 0.9:1.0

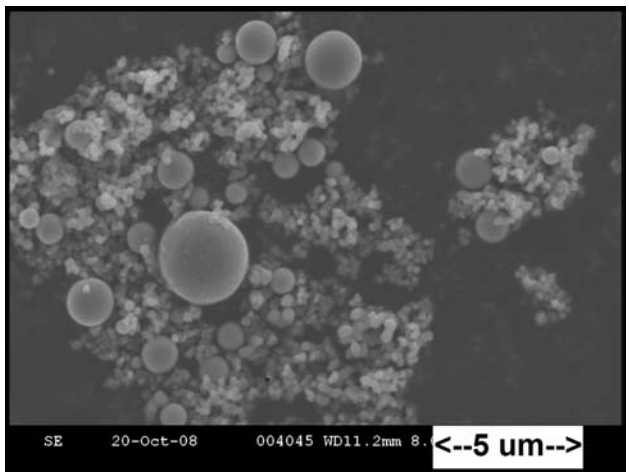

Fig. 12 SEM image of Titania particles sprayed into distilled water using setup 1. A majority of particles range in size of 50-200 nm. Setup 2 showed identical results

However, some large particles (~1 μm) were also present, which are expected due to the nature of atomization process of the precursor and leads to a broad droplet size distribution (Ref 17).

3.4 Titania Characterization

To analyze the phases of Titania present in the coatings, the liquid precursor was sprayed onto steel coupons, using both, setups 1 and 2. The spray coupons were quenched from the side opposite the coating using compressed air at 400-550 kPa. Using setup 1 it was found that the anatase phase was present at a spray distance of 200 mm. Using setup 2 it was found that the anatase phase became present at a spray distance of 150 mm.

The cooling rate of the Titania coating was controlled in order to produce the desired anatase phase, vital for its photocatalyst nature. It is understood that the transformation of metastable anatase to stable rutile phase occurs near 700 °C; therefore, it is necessary to keep the target temperature below that threshold value in order to quench the splats (Ref 5).

Previous studies have shown that when the Titania precursor is sprayed onto a steel coupon, the temperature of the coupon increases, causing a phase transformation of the Titania from anatase to rutile after deposition (Ref 5). Although the pyrolysis of the precursor in the plasma plume produces nanoparticles of Titania in anatase phase, in order to prevent the titania from stabilizing into the rutile phase the continual cooling of the steel coupon via compressed air is necessary.

The distance of the plasma gun to the steel coupon, i.e., the spray distance, also affects the phase of the titania. It has been explained that an increase in spray distance causes the liquid precursor to begin solidification in flight and maintain anatase phase titania (Ref 6). Hence, the transformation from anatase to rutile is more likely to occur once the titania has impacted the substrate. Since the axially fed precursor experiences higher temperatures than the externally fed precursor due to longer residence time in the hot core of the plasma flow, it is reasonable to expect a longer spray distance for setup 1 than for setup 2 to achieve a coating exhibiting the anatase phase in higher proportion.

The XRD patterns of the titania coatings sprayed using setups 1 and 2 are shown in Fig. 13. It can be observed that the results of setup 2 show better defined anatase peaks than setup 1. It is believed that the atomization of the precursor in setup 2, using the atomizing nozzle, outperformed the atomization of the precursor in setup 1 by the shear force of the plasma jet. The lack of atomization of the precursor in setup 1 resulted in uneven heat transfer to the precursor droplets which produced dominant rutile phase than coatings produced with setup 2.

It is to be noted that, in setup 1 spraying was done at a spray distance of 200 mm whereas in setup 2 spraying was done at a spray distance of 150 mm. Any spray distance lesser than 150 mm, causes the air cooling of the coupon to be ineffective, there by heating the sample and converting the metastable anatase into the stable rutile phase.

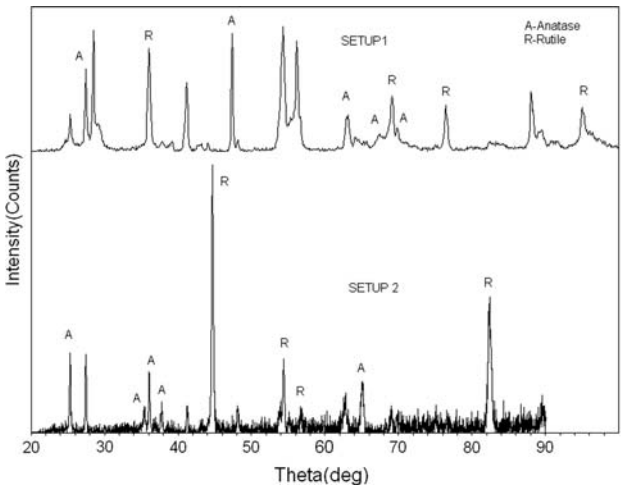

Fig. 13 XRD comparison of the Titania coatings using setups 1 and 2. Setup 1 was sprayed at a standoff distance of 8 in., whereas setup 2 was sprayed at a standoff distance of 6 in. These two coatings showed the most predominant Anatase phase

Any spray distance larger than 200 mm causes the particles to solidify before reaching the steel coupon and failing to produce an adherent coating.

3.5 Characterization of the Bulk Coating

After determining the parameters necessary to produce the constituents of the Silicon-Titania coating in the desired phases we experimented with both setups 1 and 2 to produce coatings of finely dispersed Titania nanoparticles in a Silicon matrix. From setup 1 the SEM images of the cross section of the coating are shown in Fig. 14(a) and (b) at 1000× and 6000×, respectively. From setup 2 the SEM images of the cross section of the coating are shown in Fig. 15(a) and (b) at 1000× and 6000×, respectively. From setup 2 an SEM image of the surface topology of the bulk coating is shown in Fig. 16 at 100×.

In comparison, both coatings show void content, 5.1% for setup 1 and 4.9% for setup 2, which is only slightly higher than that of the pure Silicon coatings presented in Fig. 5. Both coatings show similar surface topology (Fig. 16), however, the presence of fine particulate clusters is more apparent in setup 2 (Fig. 15a). It is clear from spherical shape of the Titania particles that they were completely melted by the plasma plume. Moreover, it can be deduced from the topology of the coatings that there was a large size distribution of the Titania particles. Some of the nano-sized particles can be seen as small clusters in the bulk material, but there were also micrometer-sized spherical Titania particles. Most importantly, using the parameters that were shown to produce the anatase phase of Titania and crystalline silicon, both setups produced coatings that dispersed Titania particles in the silicon matrix. The presence of Titania particles in the order of 100-200 nm in size was observed in coatings deposited by both the setups.

However, the coating produced by setup 1, axially feeding the precursor, showed many large strips of Titania

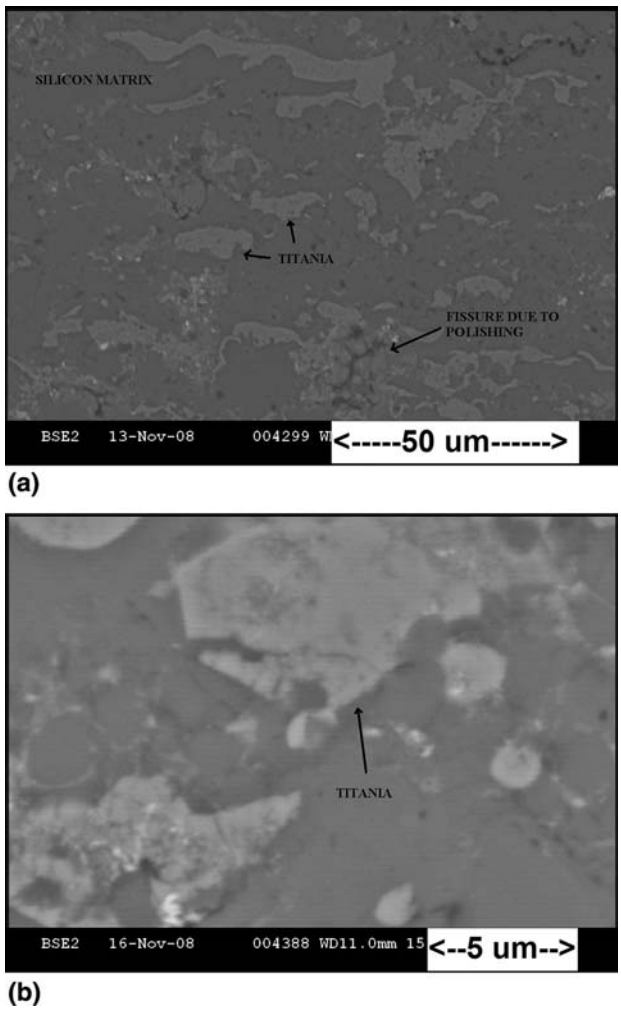

Fig. 14 (a) 1000× SEM image of the cross section of Silicon-Titania coating produced using setup 1. (b) 6000× SEM image showing Titania nanoparticles in Silicon matrix produced with setup 1

in addition to the nanoparticles of Titania. Setup 2 showed a more uniform distribution of smaller particles than setup 1. This further supports the observation that the atomization of the precursor plays a pivotal role in producing nanoparticles of Titania.

An additional factor to the production of the anatase phase is associated with the heat loss due to the silicon particles. It is to be noted that the overall power of the plasma gun in both setups that produces appropriate Silicon coating as well as anatase Titania phase was kept around 65 kW. However, while co-depositing Silicon/Titania, the much larger mass of silicon particles compared to the Titania particles, may influence the phase transformation behavior. First of all, the silicon particles will absorb a lot of energy from the plasma jet. In other words, less heat is available for the pyrolysis of the precursor. Since silicon powder is fed after the precursor injection in setup 1, the Titania particles may quench on the silicon particles and then reheat again. In setup 2 the

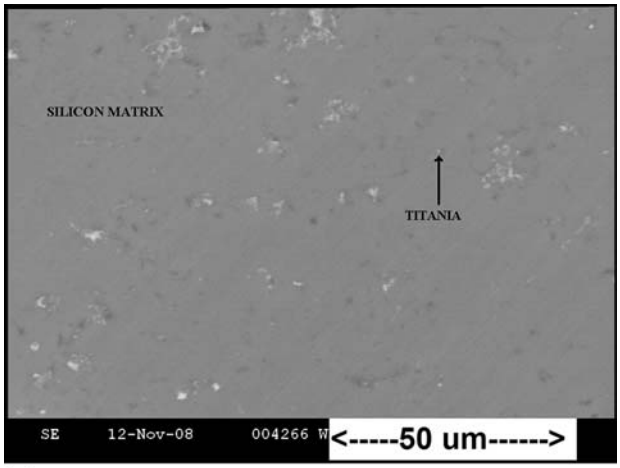

(a)

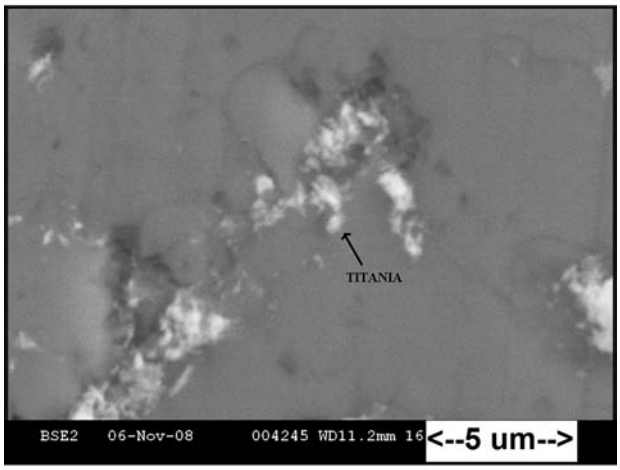

(b)

Fig. 15 (a) 1000× SEM image of the cross section of Silicon-Titania coating produced using setup 2. (b) 6000× SEM image showing Titania nanoparticles in Silicon matrix produced with setup 2

precursor particles are fed after silicon and may not go through the same temperature cycle as in the case of setup 1. Setup 2 should produce more anatase phase than the coatings in Fig. 13 which are the result of spraying purely Titania provided the target temperature is maintained below the threshold anatase-rutile transformation temperature. Verification by XRD was complicated due to the low mass fraction of Titania particles in the composite coating. The benefit of the second approach is certainly apparent in terms of particle distribution in the matrix. The ultrafine particles produced by the more efficient atomization technique of setup 2 are more evenly distributed within the plume than the particles produced by setup 1, which are larger in size. Smaller particles require less enthalpy in order to melt, and subsequently less cooling in order to quench to preserve the anatase phase. Overall, the best parameters to produce the bulk coating of nanoparticles of Titania within a silicon matrix was using 65 kW of power, 150 mm spray distance, compressed air cooling of the substrate, and externally feeding

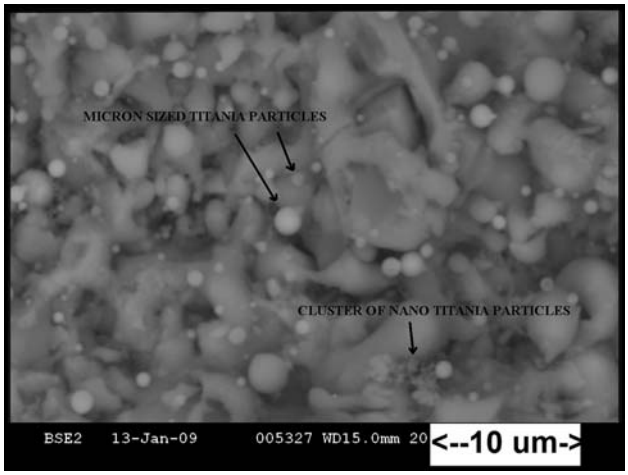

Fig. 16 1000× SEM image of bulk coating showing the surface topology using setup 1. Setup 2 yielded similar surface topology

the Titania precursor into the plasma plume using the atomizing nozzle.

4. Conclusions

The results show that the suspension plasma spray process can be used to create composite crystalline coatings of Titania nanoparticles within a Silicon matrix. Two experimental setups were operated, and the XRD and SEM results of the sprayed samples studied. The coatings were dense unlike the coatings achieved by previous studies (Ref 9-11).

It has been experimentally determined that Titania liquid precursor fed externally into a plasma plume via an atomizing nozzle will produce abundant nanoparticles of Titania in the anatase phase. Similarly, Titania precursor will produce nanoparticles of Titania in the anatase phase when fed axially into the plume of the plasma gun through the anode. In comparison, externally fed Titania precursor results show smaller particle size than axially fed Titania due to the difference in their atomization efficiency. The plasma gun parameters of 65 kW, 150 mm spray distance, compressed air cooling of the back side of the substrate, and the externally fed atomizing produced the strongest anatase phase of Titania nanoparticles within the dense silicon matrix.

Acknowledgment

Financial support from the US Navy under Contract No: N00244-07-P-0553 is gratefully acknowledged.

References

1. P.S. Shinde, S.B. Sadale, P.S. Patil, P.N. Bhosale, A. Bruger, M. Neumann-Spallart, and C.H. Bhosale, Properties of Spray Deposited Titanium Dioxide Thin Films and their Production in Photoelectrocatalysis, *Sol. Energy Mater. Sol. Cells*, 2008, **92**(3), p 283-290

2. Z. Zhang, C.-C. Wang, R. Zakaria, and J.Y. Ying, Role of Particle Size in Nanocrystalline TiO_2-based Photocatalysts, *J. Phys. Chem. B*, 1998, **102**, p 10871-10878
3. C. Lee, H. Choi, C. Lee, and H. Kim, Photocatalytic Properties of Nanostructured TiO_2 Plasma Sprayed Coating, *Surf. Coat. Technol.*, 2003, **173**, p 192-200
4. D. Chen, E.H. Jordan, M. Gell, and X. Ma, Dense TiO_2 Coating Using the Solution Precursor Plasma Spray Process, *J. Am. Ceram. Soc.*, 2008, **91**(3), p 865-872
5. C.-H. Huang, C.-H. Huang, T.-P. Nguyen, and C.-S. Hsu, Self-assembly Monolayer of Anatase Titanium Oxide from Solution Process on Indium Tin Oxide Glass Substrate for Polymer Photovoltaic Cells, *Thin Solid Films*, 2007, **15**, p 6493-6496
6. R. Jaworski, L. Pawlowski, F. Rodudet, S. Kozerski, and A. Maguer, Influence of Suspension Plasma Spraying Process Parameters on TiO_2 Coatings Microstructure, *J. Therm. Spray Technol.*, 2008, **17**(1), p 73-81
7. F.-L. Toma, G. Bertrand, D. Klein, C. Coddet, and C. Meunier, Nanostructured Photocatalytic Titania Coatings Formed by Suspension Plasma Spraying, *J. Therm. Spray Technol.*, 2006, **15**(4), p 587-592
8. Y. Zhu and C. Ding, Characterization of Plasma Sprayed Nano-Titania Coatings by Impedance Spectroscopy, *J. Eur. Ceram. Soc.*, 2000, **20**, p 127-132
9. Y. Niu, X. Liu, and C. Ding, Phase Composition and Microstructure of Silicon Coatings Deposited by Air Plasma Spraying, *Surf. Coat. Technol.*, 2006, **201**, p 1660-1665
10. J.A.M. van Roosmalen, C.J.J. Tool, R.C. Hulbert, R.J.G. Beenen, J.P.P. Huijsmans, and W.C. Sinke, Ceramic Substrates for Thin-film Crystalline Silicon Solar Cells, *Photovoltaic Specilists Conf.*, 1996, p 657-660
11. A. von Keitz, J.A.M. van Roosmalen, C.J.J. Tool, S.E.A. Schiermeier, A.J.M.M. van Zutphen, F. Fung, and G.M. Christie, Improvement of Low Cost Ceramic Substrates for use in Think Film Silicon Solar Cells, *Proceedings 2nd WCPVSEC*, 1998, p 1829-1832
12. B. Kharas, G. Wei, S. Sampath, and H. Zhang, Morphology and Microstructure of Thermal Plasma Sprayed Silicon Splats and Coatings, *Surf. Coat. Technol.*, 2006, **201**, p 1454-1463
13. I.G. Kolesnikov, B.M. Freidin, V.I. Serba, Y.V. Kuz'mich, and D.L. Rogachev, Sputtering Si-Co Alloy Targets, *Russ. Metall.*, 2008, **6**, p 529-532
14. V.M. Aroutiounian, K.S. Martirosyan, A.S. Hovhannisyan, and P.G. Soukiassian, Use of Porous Silicon for Double- and Triple-Layer Antireflection Coatings in Silicon Photovoltaic Converters, *Proc. SPIE*, 2006, **6327**, p 1-10
15. A.M. Al-Dhafiri, Crystallization of PECVD-deposited Amorphous Silicon Thin Films Using the Aluminum Induced Crystallization Technique, *J. King Saud Univ. Eng. Sci.*, 2003, **15**(2), p 235-248
16. A. Rahtu and M. Ritala, Reaction Mechanism Studies on Titanium Isopropoxide-Water Atomic Layer Deposition Process, *Chem. Vap. Deposition*, 2001, **8**(1), p 21-28
17. S. Basu, E.H. Jordan, and B.M. Cetegen, Fluid Mechanics and Heat Transfer of Liquid Precursor Droplets Injected into High-Temperature Plasmas, *J. Therm. Spray Technol.*, 2007, **17**, p 60-72